JNeurosci
THE JOURNAL OF NEUROSCIENCE

Research Articles: Systems/Circuits

Development of glutamatergic proteins in human visual cortex across the lifespan

Caitlin R. Siu[1,†], Simon P. Beshara[1,†], David G. Jones[2] and Kathryn M. Murphy[1,3]

[1]*McMaster Integrative Neuroscience Discovery and Study (MiNDS) Program, McMaster University, Hamilton ON*
[2]*Pairwise Affinity Inc, Dundas ON*
[3]*Department of Psychology, Neuroscience & Behaviour, McMaster University, Hamilton ON*

DOI: 10.1523/JNEUROSCI.2304-16.2017

Received: 20 July 2016

Revised: 30 April 2017

Accepted: 3 May 2017

Published: 29 May 2017

Author Contributions: CS Designed research, performed research, analyzed data, wrote the paper; SB designed research, performed research, analyzed data, wrote the paper; DJ analyzed data; KM designed research, analyzed data, wrote the paper.

Conflict of Interest: Authors report no conflict of interest.

We thank Kyle Hornby and Dr Joshua Pinto for technical help and Justin Balsor for comments on the manuscript.

[†]These authors contributed equally.

Funding Sources: NSERC Grant RGPIN-2015-06215 awarded to KM, Woodburn Heron OGS awarded to CS, NSERC PGS awarded to SB, and OCE awarded to DJ.

Corresponding Author: Kathryn M Murphy, Dept of Psychology Neuroscience & Behaviour, McMaster University, 1280 Main Street West, Hamilton, ON L8S 4K1, Canada, e-mail: kmurphy@mcmaster.ca

Cite as: J. Neurosci ; 10.1523/JNEUROSCI.2304-16.2017

1. Manuscript Title: Development of glutamatergic proteins in human visual cortex across the lifespan

2. Abbreviated Title: Development of human visual cortex

3. Authors: Caitlin R. Siu[1*], Simon P. Beshara[1*], David G. Jones[2], Kathryn M. Murphy[1,3]

1. McMaster Integrative Neuroscience Discovery and Study (MiNDS) Program, McMaster University, Hamilton ON
2. Pairwise Affinity Inc, Dundas ON
3. Department of Psychology, Neuroscience & Behaviour, McMaster University, Hamilton ON
* These authors contributed equally

4. Author Contributions:
CS Designed research, performed research, analyzed data, wrote the paper; SB designed research, performed research, analyzed data, wrote the paper; DJ analyzed data; KM designed research, analyzed data, wrote the paper.

5. Corresponding Author:
Kathryn M Murphy, Dept of Psychology Neuroscience & Behaviour, McMaster University, 1280 Main Street West, Hamilton, ON L8S 4K1, Canada
e-mail: kmurphy@mcmaster.ca

6. **Number of Figures:** 7

7. Number of Tables: 1

8. Number of multimedia: 0

9. Number of Words for Abstract: 243

10. Number of words for Significance Statement: 117

11. Number of words for Introduction: 494

12. Number of words for Discussion: 1640

13. Acknowledgements: We thank Kyle Hornby and Dr Joshua Pinto for technical help and Justin Balsor for comments on the manuscript.

14. Conflict of interest: Authors report no conflict of interest

15. Funding Sources: NSERC Grant RGPIN-2015-06215 awarded to KM, Woodburn Heron OGS awarded to CS, NSERC PGS awarded to SB, and OCE awarded to DJ.

Abstract

Traditionally, human primary visual cortex (V1) has been thought to mature within the first few years of life, based on anatomical studies of synapse formation, and establishment of intra- and inter-cortical connections. Human vision, however, develops well beyond the first few years. Previously, we found prolonged development of some GABAergic proteins in human V1 (Pinto et al., 2010). Yet as over 80% of synapses in V1 are excitatory, it remains unanswered if the majority of synapses regulating experience-dependent plasticity and receptive field properties develop late like their inhibitory counterparts. To address this question, we used Western blotting of post-mortem tissue from human V1 (12 female, 18 male) covering a range of ages. Then quantified a set of post-synaptic glutamatergic proteins (PSD-95, GluA2, GluN1, GluN2A, GluN2B), calculated indices for functional pairs that are developmentally regulated (GluA2:GluN1; GluN2A:GluN2B), and determined inter-individual variability. We found early loss of GluN1, prolonged development of PSD-95 and GluA2 into late childhood, protracted development of GluN2A until ~40 years and dramatic loss of GluN2A in aging. The GluA2:GluN1 index switched at ~1 year but the GluN2A:GluN2B index continued to shift until ~40 year before changing back to GluN2B in aging. We also identified young childhood as a stage of heightened inter-individual variability. The changes show that human V1 develops gradually through a series of 5 orchestrated stages, making it likely that V1 participates in visual development and plasticity across the lifespan.

Significance

Anatomical structure of human V1 appears to mature early, but vision changes across the lifespan. This discrepancy has fostered 2 hypotheses: either other aspects of V1 continue changing, or later changes in visual perception depend on extrastriate areas. Previously, we showed that some GABAergic synaptic proteins change across the lifespan but most synapses in V1 are excitatory leaving unanswered how they change. So we studied expression of glutamatergic proteins in human V1 to determine their development. Here we report prolonged maturation of glutamatergic proteins, with 5 stages that map onto life-long changes in human visual perception. Thus, the apparent discrepancy between development of structure and function may be explained by life-long synaptic changes in human V1.

Introduction

Anatomical development of human visual cortex (V1) proceeds quickly over the first few years (Huttenlocher et al., 1982; Zilles et al., 1986; Burkhalter, 1993; Burkhalter et al., 1993) but maturation of vision is slow, changing through childhood, adolescence, adulthood and aging (Kovács et al., 1999; Lewis and Maurer, 2005; Germine et al., 2011; Owsley, 2011). The discrepancy between development of structure and function led to the idea that prolonged maturation of vision might depend on features of V1 not captured by anatomical studies (Taylor et al., 2014). For example, some GABAergic and myelin proteins involved with plasticity continue developing into adulthood in human V1 (Pinto et al., 2010; Siu et al., 2015). Most V1 synapses, however, are excitatory (Beaulieu et al., 1992) and glutamatergic receptors regulate experience-dependent plasticity (Hensch, 2004; Turrigiano and Nelson, 2004; Cooper and Bear, 2012; Levelt and Hübener, 2012) and receptive field properties (Ramoa et al., 2001; Rivadulla et al., 2001; Fagiolini et al., 2004; Self et al., 2012). Currently, little is known about expression of glutamatergic proteins in human V1 (Huntley et al., 1994; Scherzer et al., 1998) and less about how they change across the lifespan (Pinto et al., 2015).

Animal models found that activation of glutamate receptors, NMDA (N-methyl-D-aspartate) and AMPA (α-amino-3-hydroxy-5-methyl-4-isoxazolepropionic acid), regulate plasticity in V1 (Kleinschmidt et al., 1987; Daw et al., 1992; Turrigiano and Nelson, 2004; Yashiro and Philpot, 2008; Smith et al., 2009; Cooke and Bear, 2014; Turrigiano, 2017). The recruitment of AMPARs to silent synapses starts the critical period (CP) (Rumpel et al., 1998) and an increase in the glutamate receptor scaffolding protein, PSD-95, consolidates synapses to end the CP (Huang et al., 2015). The composition of AMPARs and NMDARs regulates juvenile ocular dominance plasticity starting with weakening of deprived eye responses by the rapid loss of GluA2 (Heynen et al., 2003; Lambo and Turrigiano, 2013) and increase of GluN2B (Chen and Bear, 2007). Next, open eye responses are strengthened by an increase of GluA2 (Lambo and

97 Turrigiano, 2013) and decrease of GluN2A (Smith et al., 2009). The developmental shift from
98 more GluN2B to more GluN2A (2A:2B balance) regulates metaplasticity since GluN2B allows
99 more Ca2+ to enter the synapse and activate LTP mechanisms (Yashiro and Philpot, 2008). The
100 2A:2B balance shifts during the CP (Sheng et al., 1994) when visual experience drive a loss of
101 GluN2B (Philpot et al., 2001), an increase of GluN2A (Quinlan et al., 1999a; 1999b), and
102 reduces ocular dominance plasticity (Philpot et al., 2003; 2007).

103 Receptive field properties in V1 are also regulated by glutamate receptors. The dense
104 expression of glutamate receptors in layers 2/3 and 4 (Huntley et al., 1994; Kooijmans et al.,
105 2014) supports AMPARs dominated feed-forward and NMDARs dominated feed-back drive
106 (Self et al., 2012). Furthermore, development of orientation preference is prevented by
107 suppressing NMDARs (Ramoa et al., 2001) and requires the GluN2A subunit (Fagiolini et al.,
108 2003).

109 Here, we investigate development of glutamate receptors in human V1 (PSD-95, GluN1,
110 GluN2A, GluN2B and GluA2) from birth to 80 years of age. We find changes that could
111 contribute to visual processing and plasticity throughout the lifespan.

Materials and Methods

Samples

The post-mortem tissue samples from human visual cortex used in this study were obtained from the Brain and Tissue Bank for Developmental Disorders at the University of Maryland (Baltimore, MD, USA) and the study was approved by the McMaster University Research Ethics Board. Cortical samples were from individuals with no history of brain disorders, and all causes of death were with minimal trauma. Samples were collected within 23 hours post-mortem, sectioned coronally in 1cm intervals, flash frozen at the Brain and Tissue Bank, and stored at -80°C. Visual cortex samples were taken from the posterior pole of the left hemisphere and included both superior and inferior portions of the calcarine fissure. A total of 30 cases were used and ranged in age from 20 days to 79 years (Table 1).

Sample preparation

A small piece of tissue (50-100mg) was cut from the calcarine fissure of each frozen block of human V1, suspended in cold homogenization buffer (1ml buffer: 50mg tissue, 0.5mM DTT, 2mM EDTA, 2mM EGTA, 10mM HEPES, 10mg/L leupeptin, 100nM microcystin, 0.1mM PMSF, 50mg/L soybean trypsin inhibitor), and homogenized in a glass-glass Dounce hand homogenizer (Kontes, Vineland, NJ, USA). To enrich for synaptic proteins, we used a synaptosome preparation. Homogenate samples were filtered through coarse (100 μg) and fine (5 μg) pore hydrophilic mesh filters (Millipore, Bedford, MA, USA), and then centrifuged at 1000 x g for 10 minutes to obtain the synaptic fraction. The synaptosome pellet was resuspended in boiling 1% sodium-dodecyl-sulfate (SDS), heated for 10 minutes and stored at -80°C.

Synaptosome protein measurement and equating

Low abundance synaptic proteins are enriched 3- to 5-fold by the synaptosome preparation (Murphy et al., 2014) which facilitates the reliable detection of synaptic proteins by Western blot analysis. In contrast, housekeeping proteins used as loading controls, such as GAPDH or β-tubulin, are reduced about 10-fold in a synaptosome preparation because the small synaptosome

138 volume is dominated by synaptic proteins (Balsor & Murphy, unpublished observation).
139 Moreover, those loading controls are known to exhibit high variability (Lee et al., 2016) and
140 change under many conditions including experience (Dahlhaus et al., 2011) and development
141 (Pinto et al., 2015). For these reasons, normalizing an enriched synaptosome preparation with a
142 diminished loading control can lead to the undesirable outcome of inflating the apparent
143 expression of synaptic proteins, especially early in development. It is important, however, for
144 Western blot analyses to accurately quantify total protein and to load equivalent amounts. To
145 achieve these, we used a stringent 3 stage protocol to measure and equate protein concentrations
146 among the samples and then load equivalent volumes into each gel.

147 To measure and equate protein concentration for each synaptosome sample, we used a
148 bicinchoninic acid (BCA) assay (Pierce, ThermoFisher Scientific, Rockford, IL, USA) and
149 compared the samples with a set of protein standards (0.25, 0.5, 1.0, 2.0 mg/ml) (Bovine Serum
150 Albumin (BSA) protein standards, Bio-Rad Laboratories, Hercules, CA, USA). We mixed a
151 small amount of each sample and standard (9 µl) with BCA assay solution (1:100), and loaded 3
152 aliquots (each 300 µl) into separate wells of a 96-well microplate. The plate was incubated at
153 45ºC for 45 minutes to activate the reaction, then scanned in an iMark Microplate Absorbance
154 Reader (Bio-Rad Laboratories, Hercules, CA, USA) to quantify the colorimetric change. Next,
155 we plotted the absorbance values of the standards relative to their known concentrations, and fit a
156 linear correlation to the data. The fit for the correlation had to be $R^2>0.99$, and if it did not reach
157 that level, the BCA assay was re-run. The absorbance of the human samples was measured and
158 averaged for the 3 aliquots. This sample absorbance value and the linear equation fit to the
159 standards were used to determine the amount of Laemmli buffer (Cayman Chemical Company,
160 Ann Arbor, MI, USA) and sample buffer (M260 Next Gel Sample loading buffer 4x, Amresco
161 LLC, Solon, OH, USA) needed to achieve protein concentrations of 1µg/µl. Finally, to ensure
162 loading of equivalent volumes into each well of the gel we used a high-quality pipette (e.g.
163 Picus, Sartorius Corp Bohemia, NY USA) and performed regular calibrations.

Immunoblotting

Synaptosome samples (20 µg) were separated on 4-20% SDS-polyacrylamide gels (SDS-PAGE) and transferred to polyvinylidene difluoride (PVDF) membranes (Immobilon-FL PVDF, EMD Millipore, Billerica, MA, USA). Each sample was run multiple times and a control sample, made by combining a small amount of the synaptosome preparation from each of the 30 cases, was run on each gel. Blots were pre-incubated in blocking buffer for 1 hour (Odyssey Blocking Buffer 1:1 with phosphate buffer saline (PBS)) (Li-Cor Biosciences; Lincoln, NE, USA), then incubated in primary antibody overnight at 4°C using these primary antibodies: Anti-NMDAR1, 1:4000 (RRID: AB_396353, BD Pharmingen, San Jose, CA); Anti-NR2A, 1:1000 (RRID: AB_95169, EMD Millipore, Billerica, MA, USA); Anti-NMDAR2B, 1:1000 (RRID: AB_2112925, EMD Millipore, Billerica, MA, USA); Anti-GluA2, 1:1000 (RRID: AB_2533058, Invitrogen, Waltham, MA, USA); Anti-PSD95, 1:16000 (RRID: AB_94278, EMD Millipore, Billerica, MA, USA). These antibodies were selected after testing them on a multi-species blot that included samples from human, monkey, cat, and rat to ensure that the human samples had bands comparable with the other species. The blots were washed with PBS-Tween (0.05% PBS-T, Sigma, St. Louis, MO, USA) (3x10 minutes) and incubated for 1 hour at room temperature with the appropriate IRDye labeled secondary antibody, (Anti-Mouse, 1:8000, RRID: AB_10956588; Anti-Rabbit, 1:10,000, RRID: AB_621843; Li-Cor Biosciences, Lincoln, NE, USA), and washed again in PBS-Tween (3x10 minutes). The bands were visualized using the Odyssey scanner (Li-Cor Biosciences; Lincoln, NE, USA) and we determined that the amount of protein loaded into each well and the antibody concentrations were within the linear range of the Odyssey scanner. After scanning, the blots were stripped using a Blot Restore Membrane Rejuvenation Kit (EMD Millipore, Billerica, MA, USA), re-scanned to ensure complete stripping, and then re-probed with another antibody.

Band analysis

To analyze the bands, blots were scanned on an Odyssey infrared scanner and quantified using densitometry (Li-Cor Odyssey Software version 3.0; Li-Cor Biosciences; Lincoln, NE, USA). A density profile for each band was calculated by performing a subtraction of the background, integrating the pixel intensity across the area of the band, and dividing the intensity by the width of the band to control for variations in lane width. A control sample, made by combining a small amount from each sample, was run on each gel and the density of each sample was quantified relative to the control (sample density/control density).

Band image manipulation

Bands shown on figures are representative samples and were added to the figures in Photoshop (Adobe Systems Inc, San Jose, CA, USA, RRID:SCR_014199). Horizontal and vertical transformations were applied to size and orient the bands for each figure. A linear adjustment layer was applied uniformly to all bands for each protein, preserving the relative intensities among bands.

Receptor subunit index

To quantify the balance between functional pairs of proteins, we calculated a difference ratio, often called a contrast index, that is commonly used in signal processing to determine the quality of a signal. We calculated 2 indices that reflect the balance between pairs of proteins that are developmentally regulated: AMPA:NMDA index -- (GluA2-GluN1)/(GluA2+GluN1); and NMDAR subunit 2A:2B index -- (GluN2A-GluN2B)/(GluN2B+GluN2A). These indices can have values between -1 and +1.

Curve-fitting and statistical analyses

The results were plotted in two ways to visualize and analyze changes in expression across the lifespan. First, to describe the time course of changes in protein expression, scatterplots were made for each protein showing the expression level from each run (grey dots) and the average of the runs (black dots). To determine the trajectory of changes across the lifespan we used a

model-fitting approach (Christopoulos and Lew, 2000) and found the best curve-fit to the data using Matlab (The MathWorks, Inc, Natick, MA, RRID: SCR_001622). A single-exponential decay function ($Y=A*\exp(-(x/\tau))+B$) was fit to the data for GluN1. A Gaussian function ($Y=A*\exp(-((\log(x/\mu)^2)/(2*(\sigma^2)))+B$) was fit to the data for PSD-95, GluA2, GluN2B, and the 2A:2B index. A quadratic function was fit to the AMPA:NMDA balance ($Y=A+B*\log(x)+C*\log(x)^2$). Finally, a weighted average was used to describe the trajectory for GluN2A. The fits were found by least squares, and the goodness-of-fit (R^2) and statistical significance of the fit (p) were determined. For the decay function, we calculated the time constants (τ) and defined 3τ (when 87.5% of the change in expression had occurred) as the age when mature expression was reached with the 95% confidence interval (95% CI) around that age. For Gaussian functions, the age at the peak was calculated and the 95% CI determined.

Second, to compare changes among different stages across the lifespan, samples were binned into age groups (<0.3 years, Neonates; 0.3-1 year, Infants; 1-4 years, Young Children; 5-11 years, Older Children; 12-20 years, Teens; 21-55 years, Young Adults; >55 years, Older Adults) and histograms were plotted showing the mean and standard error of the mean (SEM) for each group. We used bootstrapping to make statistical comparisons among the groups since this method provides robust estimates of standard error and CI, which are especially useful for human studies constrained to smaller sample sizes. The statistical software R (R Core Team (2014), R: A language and environment for statistical computing. R Foundation for Statistical Computing, Vienna, Austria, URL http://www.R-project.org/, RRID: SCR_001905) was used for the bootstrapping and we began by simulating a normally distributed dataset (1,000,000 points) with the same mean and standard deviation of the group being compared. We used this normally distributed dataset to determine if the observed means for the other age groups were significantly different. A Monte Carlo simulation was used to randomly sample from the simulated dataset N times, where N was the number of cases in the other age groups. This simulation was run 10,000 times to generate an expected distribution for the N number of cases. Confidence intervals (CI)

were calculated for that simulated distribution (i.e. 95%, 99% CI) and compared with the observed group means. The age groups were considered to be significantly different (i.e. $p<0.05$) when the observed mean was outside the 95% CI.

Analysis of Inter-individual variability

Previously we identified ages during infancy and childhood with waves of high inter-individual variability (Pinto et al., 2015; Siu et al., 2015). To analyze if the glutamatergic proteins studied here have similar waves of inter-individual variability we calculated the Fano-Factor (Variance-to-Mean Ratio - VMR) for each protein and examined how it changed across the lifespan. The VMR around each case was determined by calculating the mean and variance for the protein expression within a moving box that included 3 adjacent ages and then dividing the variance by the mean. Scatter plots were made to show how the VMRs changed across the life span and functions were fit to those data to identify ages when there was high inter-individual variability. The VMRs were fit with the same Gaussian function described above, and a wave of higher inter-individual variability was identified when 4 or more points at the peak fell above the 95% CI for lower bound of the curve.

Results

Postmortem interval

We examined whether glutamate protein expression levels were affected by post-mortem interval (PMI). First, we verified that immunoreactivity was present and then analyzed the correlation between PMI and protein expression. There were no significant correlations between PMI and expression of the 5 glutamatergic proteins (PSD-95: R=0.05, p=0.66; GluA2: R=0.17, p=0.13; GluN1: R=0.26, p=0.11; GluN2A: R=0.17, p=0.41; GluN2B: R=0.16, p=0.24) so all of the data was included in the following analyses.

Slow development of PSD-95, earlier but opposite development of GluA2 and GluN1

We began analyzing development of glutamate proteins in human V1 by measuring expression of PSD-95, a scaffolding protein involved in anchoring AMPA and NMDA receptors (Kim and Sheng, 2004), controlling visual developmental plasticity (Yoshii et al., 2003), and ending the CP for ocular dominance plasticity (Huang et al., 2015). We found a steady increase in expression of PSD-95 in the synaptosome preparation used in this study and analyzed the results in two ways (Fig. 1). First, by model-fitting to all the data to determine the best curve to capture changes across the lifespan, and second, by binning the data into age groups and using bootstrapping for statistical comparisons between groups. Development of PSD-95 peaked at 9.6 years (+/- 4.1 years; R^2=0.457, p<0.0001) (Fig. 1A). This result was similar to our previous findings using whole homogenate samples (Pinto et al., 2015). The magnitude of the peak in the synaptosome, however, was about half that found using the whole homogenate ((Pinto et al., 2015) figure 3), suggesting there could be a large mobile pool of PSD-95 during late childhood. Comparing the age-binned results showed a 3-fold increase in PSD-95 expression during development that reached a peak in older children (5-11 years, p<0.001) before dropping about 30% into aging (p<0.001) (Fig. 1B). The PSD-95 peak corresponded with the age when children are no longer susceptible to amblyopia (Lewis and Maurer, 2005) and may signify that PSD-95

281 contributes to ending the CP for ocular dominance plasticity in humans similar to its role in rat
282 V1 (Huang et al., 2015).

283 Next, we quantified development of GluA2 and GluN1, which identify the 2 main classes of
284 ionotropic glutamate receptors AMPARs and NMDARs, respectively. Development of these
285 subunits followed a similar pattern to that found in animal studies, where GluA2 increased, while
286 GluN1 decreased during development (Fig. 1C-F). GluA2 expression increased about 40%
287 during childhood and then declined a similar amount into adulthood and aging. The GluA2
288 developmental trajectory peaked at 3.1 years (+/- 1.8 years, R^2=0.131, $p<0.01$) (Fig. 1C).
289 Comparison of GluA2 expression among the age groups, however, identified a slightly later peak
290 during late childhood (5-11 years) (Fig. 1D). The uncertainty about the peak for GluA2 probably
291 reflects variability in expression during childhood and the modest increase between neonates and
292 older children.

293 The trajectory of GluN1 expression started high under 1 year of age, then rapidly decreased to
294 a relatively constant level for the rest of the lifespan (Fig. 1E,F). The change in GluN1
295 expression was fit with an exponential decay function (R^2=0.482, $p<0.0001$) that fell to mature
296 levels (3τ) by 4.2 years (+/- 1.7 years) (Fig. 1E). The same pattern was found when we
297 compared among age groups where GluN1 levels were higher under 1 year and dropped by
298 almost half during young childhood (1-4 years) ($p<0.001$) and remained at that level for the rest
299 of the lifespan (Fig. 1F).

300 Comparing the changes across the lifespan for PSD-95, GluA2, and GluN1 we found different
301 timing (GluA2 and GluN1 matured before PSD-95), different directions (PSD-95 and GluA2
302 increased while GluN1 decreased), and different amounts of protein change. Thus, even these 3
303 tightly associated proteins had different developmental trajectories.

Early shift from more NMDA to more AMPA in human V1

Animal studies have shown that there is an early developmental shift from NMDAR-dominated silent synapses to functional synapses with AMPARs (Isaac et al., 1997; Rumpel et al., 1998). Here we examined development of the AMPA:NMDA balance in human V1 as an indication of functional maturation of glutamatergic transmission. We calculated an AMPA:NMDA index where a value of -1 indicated only GluN1 expression, 0 indicated equal expression, and +1 indicated only GluA2 expression. We found an early switch from more GluN1 under 1 year of age to more GluA2 after 1 year (Fig. 2). The AMPA:NMDA balance was fit with a quadratic function (R^2=0.406, $p<0.0001$) that captured the shift from GluN1 to GluA2 that peaked at 10.7 years (95%CI 4.8-23.7 years) before slowly returning to equal expression during aging (Fig. 2A). The age-binned results showed the same pattern of a significant switch at 1 year, GluA2 peaking during late childhood, and returning to balanced expression in older adults (Fig. 2B). The changes in this AMPA:NMDA balance suggest an early stage of human V1 development during infancy (<1 year) that may characterize unsilencing of glutamate synapses followed by AMPAR dominated excitatory drive during childhood and young adults before regressing to balanced AMPAR and NMDAR expression in aging.

GluN2A and GluN2B subunit expression in human V1

We examined developmental changes in expression of 2 NMDAR subunits, GluN2A and GluN2B because they affect development of receptive field tuning and ocular dominance plasticity. In particular, the rise of GluN2A and concomitant loss of GluN2B during the CP is one mechanism that causes reduced ocular dominance plasticity in adult cortex (Philpot et al., 2007). The scatterplot of GluN2B expression showed a modest peak during childhood and relatively constant expression through teens, young adults, and older adults (Fig. 3A&B). The GluN2B trajectory was fit by a Gaussian function (R^2=0.176, $p<0.01$) that peaked at 1.2 years (+/- 0.7 years) (Fig. 3A). We compared GluN2B expression among the age groups and found

higher levels during childhood (5-11 years) relative to teens, young adults, and older adults (Fig. 3B) ($p<0.01$).

The developmental trajectory for GluN2A was different from GluN2B. Initially, GluN2A expression was low, then variable during childhood and teenage years (8 cases with low and 3 cases with high GluN2A expression) followed by high expression in young adults and ending with a large (~75%) decline into aging. The variability during childhood reduced the goodness-of-fit for a Gaussian function so instead we plotted a descriptive weighted curve (Fig. 3C). Interestingly, the 3 childhood cases with high GluN2A expression also had high GluN2B expression. Binning the results into age groups showed that young adults had more GluN2A expression than infants ($p<0.001$), young children ($p<0.01$), teens ($p<0.01$), and older adults ($p<0.001$) (Fig 3. D).

NMDARs are tetrameric channels with diheteromeric nascent receptors comprised of GluN1/GluN2B that shift during development with the majority becoming triheteromers comprised of GluN1/GluN2A/GluN2B (Sheng et al., 1994). Since GluN1 is a component of all NMDARs we normalized expression of GluN2A and GluN2B to the expression of GluN1 to determine if high variability during childhood was driven by variability in the total pool of NMDARs. Normalizing with GluN1 expression reduced the variability for both GluN2A and GluN2B throughout childhood, it also enhanced the GluN2B peak in late childhood (Fig. 4 A&B) and the GluN2A peak in adulthood (Fig. 4 C&D). The GluN1 normalization, however, did not eliminate variability of GluN2A and GluN2B during childhood.

2A:2B balance: protracted change across the lifespan

Visual experience shifts the 2A:2B balance in favour of GluN2A (Quinlan et al., 1999a; 1999b) and that regulates the synaptic modification threshold for engaging long-term potentiation (LTP) versus long-term depression (LTD) (Philpot et al., 2007). Since the 2A:2B balance is a key mechanism regulating visual experience-dependent metaplasticity, we analyzed

it for human V1 by calculating an index of 2A:2B expression for each case. Here we found an orderly progression from more GluN2B under 5 years of age, to roughly balanced GluN2B and GluN2A during the teen years, to a peak with more GluN2A during adulthood, followed by a shift back to more GluN2B in aging (Fig. 5 A&B). These changes in the 2A:2B balance were fit by a Gaussian function (R^2=0.633, p<0.0001) that peaked at 35.9 years (+/- 4.6 years) (Fig. 5A). The binned results illustrate the progressive shift towards significantly more GluN2A in adulthood and then shifting back to GluN2B in aging (Fig. 5B). The orderly shift in the 2A:2B balance, especially through childhood, was somewhat surprising since the individual subunits showed a lot of variability at that stage. The low variability of the 2A:2B index suggests that the balance between this pair of subunits, rather than the absolute amount of each, is a critical component for GluN2A and GluN2B regulation of developmental plasticity. Importantly, when compared with animal models where the shift to GluN2A is complete by the end of the CP (Sheng et al., 1994; Quinlan et al., 1999a; Beston et al., 2010), the 2A:2B shift in human V1 continued for 25 years beyond the age for susceptibility of developing amblyopia (Lewis and Maurer, 2005).

Waves of inter-individual variability during childhood

Many studies of human brain development and function have found large inter-individual variations including our studies of synaptic and non-synaptic proteins in human V1. We analyzed inter-individual variability and found waves of higher variability in childhood (Pinto et al., 2015; Siu et al., 2015). Here we applied the same approach and calculated the Fano factor to determine how the variance-to-mean ratio (VMR) changed across the lifespan for the current set of glutamatergic proteins.

We found that each glutamatergic protein had a wave of higher inter-individual variability during childhood that was well fit by a Gaussian function (Fig. 6 A-E). There was a progression in the peak age of inter-individual variability (VMRs) that began with GluN1 and GluN2B at 1.1 years (GluN1, +/- 0.2 years, R^2= 0.8, p < 0.0001)(GluN2B, +/- 0.3 years, R^2= 0.618, p < 0.0001),

to GluN2A at 1.6 years (+/- 0.4 years, R^2= 0.694, $p < 0.0001$), to GluA2 at 2.1 years (+/- 0.6 years, R^2= 0.641, $p < 0.0001$), to PSD-95 at 2.5 years (+/- 0.5 years, R^2= 0.778, $p < 0.0001$) (Fig 6 A-E). We plotted the progression of peak ages for inter-individual variability with their 95% CIs to show that variability occurred between 1-3 years of age and the peaks started with GluN1 and GluN2B then progressed to GluN2A, GluA2 and ended with PSD-95 (Fig. 6F).

Discussion

Our results show that development of glutamatergic synaptic proteins in human V1 mirror changes in visual perception across the lifespan. Human visual perception matures in stages (Ellemberg et al., 1999; Kovács et al., 1999; Braddick et al., 2005; Owsley, 2011; Hartshorne and Germine, 2015), and the glutamate receptor proteins studied here revealed 5 stages of development (Fig. 7). Those stages can support structural maturation of the intrinsic network, visually driven plasticity, closure of the CP, synaptic stability, and degeneration in human V1. These results are similar to the maturation of GABAergic proteins in human V1 (Pinto et al., 2010) and suggest that synaptic changes in V1 are likely to impact visual perception and plasticity across the lifespan.

Glutamatergic proteins regulate fundamental aspects of excitatory neurotransmission (Cull-Candy et al., 1998), visual plasticity (Turrigiano, 2008; Yashiro and Philpot, 2008; Cooke and Bear, 2014; Turrigiano, 2017), and receptive field properties in V1 (Ramoa et al., 2001; Rivadulla et al., 2001; Fagiolini et al., 2004; Self et al., 2012). Quantification of these proteins by Western blotting is one of the few methods that can track the maturation of human V1 to link changes in synaptic function, network structure, and visual perception. Protein analysis, however, does not address the cell types, layers, and circuits that are changing. Nor does it separate pre- and post-synaptic NMDARs which play different roles in neurotransmission and experience-dependent plasticity (Banerjee et al., 2016). The current results may provide a blueprint to focus anatomical and other studies of human V1 on key stages of development.

Five stages of glutamatergic protein development in human V1

Stage 1: the first year -- structural maturation of the intrinsic network

Initially, GluN1 expression was high and then a rapid reduction at ~1 year caused a switch in the AMPA:NMDA balance to more GluA2. That pattern suggests initial dominance by NMDAR-containing silent synapses that are rapidly replaced by AMPAR-containing active

410 synapses (Isaac et al., 1997; Rumpel et al., 1998). The loss of GluN1 at ~1 year coincides with a
411 loss of the endocannabinoid receptor CB1 (Pinto et al., 2010) and since CB1 plays a central role
412 in establishing excitatory connections (Harkany et al., 2008), the high levels of CB1 and GluN1
413 may contribute to the functional maturation of intra-cortical (Burkhalter et al., 1993) and inter-
414 cortical connections (Burkhalter, 1993).

415 We found that GluN2B dominated the 2A:2B balance throughout stages 1 to 3. Many animal
416 studies have shown that the 2A:2B balance contributes to developmental plasticity in V1 and
417 emergence of visual function (Quinlan et al., 1999a; Erisir and Harris, 2003; Philpot et al., 2007;
418 Cho et al., 2009; Smith et al., 2009; Durand et al., 2012). The dominance of GluN2B suggests
419 that the synaptic modification threshold favors LTP (Philpot et al., 2007; Yashiro and Philpot,
420 2008) and V1 neurons are more receptive to potentiation of an open eye's inputs (Cho et al.,
421 2009). This may explain why just 1 hour of visual experience in an infant is enough to improve
422 acuity of an eye treated for congenital cataracts (Maurer et al., 1999). Thus, this stage reflects
423 the establishment of nascent excitatory synapses and initiation of plasticity in V1 circuits.

424 **Stage 2: young children (1-4 years) -- visually driven plasticity**

425 During the second stage of V1 development, we found progressive increases in GluA2, PSD-
426 95, and GluN2A but the dominant feature was the wave of inter-individual variability. The
427 variability was similar to our previous findings for pre- (Synapsin, Synaptophysin), post-synaptic
428 (Gephyrin, PSD-95), and a non-neuronal protein (Golli myelin basic protein, MBP) (Pinto et al.,
429 2015; Siu et al., 2015). Variability peaking with GluN1 and GluN2B at ~1 year, GluN2A at ~1.5
430 years, GluA2 at ~2 years, and ending with PSD-95 at ~2.5 years. Those waves may reflect true
431 inter-individual variability in young children with cortical development taking off at different
432 ages. The waves may also represent high levels of intra-individual variability driven by the
433 dynamics of network states where expression of each synaptic protein could be high one day and
434 low the next. Since the data here are cross-sectional, we cannot differentiate between these 2

435 ideas, but the implications for them on cortical development are different. For example, if the
436 waves reflect on-going dynamics then they could function similar to how feedback about the
437 network state shifts processing of olfactory circuits in C. elegans (Gordus et al., 2015). In that
438 model, environmental or other factors could modulate the state of synaptic plasticity. Rather
439 than thinking about the waves as random or unpredictable, they may reveal a feature of visually
440 driven plasticity needed to develop adaptive circuits that support visual processing.

441 **Stage 3: older children (5-11 years) -- closure of the critical period**

442 Expression of GluN2B, PSD-95, GluA2 and the AMPA:NMDA balance peaked in the third
443 stage. These changes could end the CP for ocular dominance plasticity (Erisir and Harris, 2003;
444 Huang et al., 2015). For example, in mouse V1 PSD-95 ipeaks at the end of the CP and
445 consolidates AMPA-containing synapses (Huang et al., 2015). This stage also coincides with the
446 end of susceptibility for children developing amblyopia (Epelbaum et al., 1993; Keech and
447 Kutschke, 1995; Lewis and Maurer, 2005).

448 By the end of stage 3, the 2A:2B balance was roughly equal. A shift to more GluN2A in V1
449 is driven by visual experience (Quinlan et al., 1999b) and the findings here show that the 2A:2B
450 shift begins in young children, but is still not complete by the end of the CP for developing
451 amblyopia. In contrast, the 2A:2B shift in animal models is complete by the end of the CP
452 (Sheng et al., 1994; Quinlan et al., 1999a; Beston et al., 2010). Perhaps the slow 2A:2B shift in
453 combination with peak expression of GluA2 allows for strong engagement of both Hebbian and
454 homeostatic forms of experience-dependent plasticity (Turrigiano, 2017).

455 **Stage 4: teens and young adults (12-55 years) -- synaptic stability**

456 Through teens and young adults there was continued development as the 2A:2B balance
457 switched to favor GluN2A and peak expression of GluN2A did not occur until ~40 years. This
458 may seem like surprisingly slow development for human V1, but it was comparable to the

development of some GABAergic proteins (GAD65 and $GABA_A\alpha1$) (Pinto et al., 2010) as well as cortical myelin (classic-MBP) (Siu et al., 2015).

In mouse V1, the developmental shift to more GluN2A is slower for parvalbumin-positive (PV+) inhibitory interneurons than pyramidal neurons (Mierau et al., 2016). Perhaps the slow 2A:2B shift in human V1 reflects late maturation of PV+ cells. Fast-spiking PV+ cells also have GluA2-containing AMPARs (Kooijmans et al., 2014), so they are a site where changes in visual experience could activate inhibitory and excitatory aspects of short-term plasticity in human V1 (Lunghi 2011) (Lunghi et al., 2015a; 2015b). Interestingly, blocking NMDARs prevents surround-suppression in monkey V1 (Self et al., 2012) and even a low dose of the non-competitive NMDAR antagonist, ketamine, impairs the performance of human observers on a spatial integration task (Meuwese et al., 2013).

The late 2A:2B shift is likely to adjust the synaptic modification threshold making it more difficult for visual experience to engage LTP (Yashiro and Philpot, 2008). More GluN2A will also shorten the decay time of NMDARs (Stocca and Vicini, 1998; Vicini et al., 1998) even for triheteromeric receptors (Hansen et al., 2014). In addition, GluN2A-containing NMDARs are more stable in the synapse (Groc et al., 2006) and their activation promotes cell survival (Liu et al., 2007). These features of GluN2A-containing receptors suggests that this stage reflects a time of synaptic stability in human V1.

Stage 5: aging (>55 years) -- degeneration

The last stage saw a dramatic ~75% loss of GluN2A expression, bringing it back to levels found in infants (<1 year of age). In contrast, there was no change in GluN2B expression so the 2A:2B balance switched back to GluN2B in aging.

Age-related changes in human vision (Bennett et al., 2007; Betts et al., 2007) and monkey receptive field properties (Leventhal et al., 2003; Wang et al., 2005; Zhang et al., 2008) have

been described as resulting from poor signal-to-noise caused by a loss of inhibition. Our previous study of GABAergic proteins in human V1 found a modest loss of GAD65 (Pinto et al., 2010), but that was much less than the loss of GuN2A found here. Since GluN2A-containing NMDARs are dense on PV+ inhibitory interneurons in young mice (Mierau et al., 2016), the loss of GluN2A in aging human V1 may involve PV+ cells.

The age-related 2A:2B shift to more GluN2B is likely to cause slower decay times and weaker conductances at NMDARs (Cull-Candy et al., 1998; Vicini et al., 1998; Hansen et al., 2014). It could also slide the synaptic modification threshold so that visual experience can more readily engage LTP. That plasticity, however, may come at the cost of higher metabolic stress, GluN2B-activated excitotoxicity (Liu et al., 2007) and other vulnerabilities linked with NMDARs changes in aging (Magnusson et al., 2010). It is clear that the aging cortex does not simply become juvenile-like (Williams et al., 2010) and the specific loss of GluN2A found here could be a harbinger of degeneration in human V1.

Summary

The current results and our other investigations of human V1 show that synaptic and non-synaptic proteins develop through a series of orchestrated stages that extend across the lifespan (Murphy et al., 2005; Pinto et al., 2010; Williams et al., 2010; Pinto et al., 2015; Siu et al., 2015). The glutamatergic proteins studied here are central players in visually-driven plasticity, receptive field properties, and visual function. We found a late shift in the 2A:2B balance and a gradual maturation of GluA2. These findings will enable researchers to test the efficacy of specific neuroplasticity-based therapies at different stages of the lifespan.

References

Banerjee A, Larsen RS, Philpot BD, Paulsen O (2016) Roles of Presynaptic NMDA Receptors in Neurotransmission and Plasticity. Trends in Neurosciences 39:26–39.

Beaulieu C, Kisvarday Z, Somogyi P, Cynader M, Cowey A (1992) Quantitative distribution of GABA-immunopositive and-immunonegative neurons and synapses in the monkey striate cortex (area 17). Cereb Cortex 2:295–309.

Bennett PJ, Sekuler R, Sekuler AB (2007) The effects of aging on motion detection and direction identification. VISION RESEARCH 47:799–809.

Beston BR, Jones DG, Murphy KM (2010) Experience-dependent changes in excitatory and inhibitory receptor subunit expression in visual cortex. Front Synaptic Neurosci 2:138.

Betts LR, Sekuler AB, Bennett PJ (2007) The effects of aging on orientation discrimination. VISION RESEARCH 47:1769–1780.

Braddick O, Birtles D, Wattam-Bell J, Atkinson J (2005) Motion- and orientation-specific cortical responses in infancy. VISION RESEARCH 45:3169–3179.

Burkhalter A (1993) Development of Forward and Feedback Connections between Areas V1 and V2 of Human Visual Cortex. Cereb Cortex 3:476–487.

Burkhalter A, Bernardo KL, Charles V (1993) Development of local circuits in human visual cortex. J Neurosci 13:1916–1931.

Chen WS, Bear MF (2007) Activity-dependent regulation of NR2B translation contributes to metaplasticity in mouse visual cortex. Neuropharmacology 52:200–214.

525 Cho KKA, Khibnik L, Philpot BD, Bear MF (2009) The ratio of NR2A/B NMDA receptor
526 subunits determines the qualities of ocular dominance plasticity in visual cortex.
527 Proceedings of the National Academy of Sciences 106:5377–5382.

528 Christopoulos A, Lew MJ (2000) Beyond eyeballing: fitting models to experimental data. Crit
529 Rev Biochem Mol Biol 35:359–391.

530 Cooke SF, Bear MF (2014) How the mechanisms of long-term synaptic potentiation and
531 depression serve experience-dependent plasticity in primary visual cortex. Philosophical
532 Transactions of the Royal Society B: Biological Sciences 369:20130284–20130284.

533 Cooper LN, Bear MF (2012) The BCM theory of synapse modification at 30: interaction of
534 theory with experiment. Nat Rev Neurosci 13:798–810.

535 Cull-Candy SG, Brickley SG, Misra C, Feldmeyer D, Momiyama A, Farrant M (1998) NMDA
536 receptor diversity in the cerebellum: identification of subunits contributing to functional
537 receptors. Neuropharmacology 37:1369–1380.

538 Dahlhaus M, Li KW, van der Schors RC, Saiepour MH, van Nierop P, Heimel JA, Hermans JM,
539 Loos M, Smit AB, Levelt CN (2011) The synaptic proteome during development and
540 plasticity of the mouse visual cortex. Mol Cell Proteomics 10:M110.005413–
541 M110.005413.

542 Daw NW, Fox K, Sato H, Czepita D (1992) Critical period for monocular deprivation in the cat
543 visual cortex. Journal of Neurophysiology 67:197–202.

544 Durand S, Patrizi A, Quast KB, Hachigian L, Pavlyuk R, Saxena A, Carninci P, Hensch TK,
545 Fagiolini M (2012) NMDA receptor regulation prevents regression of visual cortical
546 function in the absence of Mecp2. Neuron 76:1078–1090.

547 Ellemberg D, Lewis TL, Liu CH, Maurer D (1999) Development of spatial and temporal vision
548 during childhood. VISION RESEARCH 39:2325–2333.

549 Epelbaum M, Milleret C, Buisseret P, Dufier JL (1993) The sensitive period for strabismic
550 amblyopia in humans. Ophthalmology 100:323–327.

551 Erisir A, Harris JL (2003) Decline of the critical period of visual plasticity is concurrent with the
552 reduction of NR2B subunit of the synaptic NMDA receptor in layer 4. Journal of
553 Neuroscience 23:5208–5218.

554 Fagiolini M, Fritschy J-M, Löw K, Möhler H, Rudolph U, Hensch TK (2004) Specific GABAA
555 circuits for visual cortical plasticity. Science 303:1681–1683.

556 Fagiolini M, Katagiri H, Miyamoto H, Mori H, Grant SGN, Mishina M, Hensch TK (2003)
557 Separable features of visual cortical plasticity revealed by N-methyl-D-aspartate receptor
558 2A signaling. Proc Natl Acad Sci U S A 100:2854–2859.

559 Germine LT, Duchaine B, Nakayama K (2011) Where cognitive development and aging meet:
560 face learning ability peaks after age 30. Cognition 118:201–210.

561 Gordus A, Pokala N, Levy S, Flavell SW, Bargmann CI (2015) Feedback from network states
562 generates variability in a probabilistic olfactory circuit. Cell 161:215–227.

563 Groc L, Heine M, Cousins SL, Stephenson FA, Lounis B, Cognet L, Choquet D (2006) NMDA
564 receptor surface mobility depends on NR2A-2B subunits. Proc Natl Acad Sci U S A
565 103:18769–18774.

566 Hansen KB, Ogden KK, Yuan H, Traynelis SF (2014) Distinct functional and pharmacological
567 properties of Triheteromeric GluN1/GluN2A/GluN2B NMDA receptors. Neuron
568 81:1084–1096.

569 Harkany T, Mackie K, Doherty P (2008) Wiring and firing neuronal networks: endocannabinoids
570 take center stage. Current Opinion in Neurobiology 18:338–345.

571 Hartshorne JK, Germine LT (2015) When does cognitive functioning peak? The asynchronous
572 rise and fall of different cognitive abilities across the life span. Psychol Sci 26:433–443.

573 Hensch TK (2004) Critical period regulation. Annu Rev Neurosci 27:549–579.

574 Heynen AJ, Yoon B-J, Liu C-H, Chung HJ, Huganir RL, Bear MF (2003) Molecular mechanism
575 for loss of visual cortical responsiveness following brief monocular deprivation. Nat
576 Neurosci 6:854–862.

577 Huang X, Stodieck SK, Goetze B, Cui L, Wong MH, Wenzel C, Hosang L, Dong Y, Löwel S,
578 Schlüter OM (2015) Progressive maturation of silent synapses governs the duration of a
579 critical period. Proceedings of the National Academy of Sciences 112:E3131–E3140.

580 Huntley GW, Vickers JC, Janssen W, Brose N, Heinemann SF, Morrison JH (1994) Distribution
581 and synaptic localization of immunocytochemically identified NMDA receptor subunit
582 proteins in sensory-motor and visual cortices of monkey and human. J Neurosci 14:3603–
583 3619.

584 Huttenlocher PR, de Courten C, Garey LJ, Van der Loos H (1982) Synaptogenesis in human
585 visual cortex--evidence for synapse elimination during normal development.
586 Neuroscience Letters 33:247–252.

587 Isaac JT, Crair MC, Nicoll RA, Malenka RC (1997) Silent synapses during development of
588 thalamocortical inputs. Neuron 18:269–280.

589 Keech RV, Kutschke PJ (1995) Upper age limit for the development of amblyopia. J Pediatr
590 Ophthalmol Strabismus 32:89–93.

591 Kim E, Sheng M (2004) PDZ domain proteins of synapses. Nat Rev Neurosci 5:771–781.

592 Kleinschmidt A, Bear MF, Singer W (1987) Blockade of "NMDA" receptors disrupts
593 experience-dependent plasticity of kitten striate cortex. Science 238:355–358.

594 Kooijmans RN, Self MW, Wouterlood FG, Beliën JAM, Roelfsema PR (2014) Inhibitory
595 interneuron classes express complementary AMPA-receptor patterns in macaque primary
596 visual cortex. Journal of Neuroscience 34:6303–6315.

597 Kovács I, Kozma P, Fehér A, Benedek G (1999) Late maturation of visual spatial integration in
598 humans. Proc Natl Acad Sci U S A 96:12204–12209.

599 Lambo ME, Turrigiano GG (2013) Synaptic and intrinsic homeostatic mechanisms cooperate to
600 increase L2/3 pyramidal neuron excitability during a late phase of critical period
601 plasticity. Journal of Neuroscience 33:8810–8819.

602 Lee H-G, Jo J, Hong H-H, Kim KK, Park J-K, Cho S-J, Park C (2016) State-of-the-art
603 housekeeping proteins for quantitative western blotting: Revisiting the first draft of the
604 human proteome. Proteomics 16:1863–1867.

605 Levelt CN, Hübener M (2012) Critical-period plasticity in the visual cortex. Annu Rev Neurosci
606 35:309–330.

607 Leventhal AG, Wang Y, Pu M, Zhou Y, Ma Y (2003) GABA and its agonists improved visual
608 cortical function in senescent monkeys. Science Signalling 300:812.

609 Lewis TL, Maurer D (2005) Multiple sensitive periods in human visual development: Evidence
610 from visually deprived children. Dev Psychobiol 46:163–183.

611 Liu Y, Wong TP, Aarts M, Rooyakkers A, Liu L, Lai TW, Wu DC, Lu J, Tymianski M, Craig
612 AM, Wang YT (2007) NMDA receptor subunits have differential roles in mediating

613 excitotoxic neuronal death both in vitro and in vivo. Journal of Neuroscience 27:2846–
614 2857.

615 Lunghi C, Berchicci M, Morrone MC, Di Russo F (2015a) Short-term monocular deprivation
616 alters early components of visual evoked potentials. The Journal of Physiology
617 593:4361–4372.

618 Lunghi C, Emir UE, Morrone MC, Bridge H (2015b) Short-term monocular deprivation alters
619 GABA in the adult human visual cortex. Curr Biol 25:1496–1501.

620 Magnusson KR, Brim BL, Das SR (2010) Selective Vulnerabilities of N-methyl-D-aspartate
621 (NMDA) Receptors During Brain Aging. Front Aging Neurosci 2:11.

622 Maurer D, Lewis TL, Brent HP, Levin AV (1999) Rapid improvement in the acuity of infants
623 after visual input. Science 286:108–110.

624 Meuwese JDI, van Loon AM, Scholte HS, Lirk PB, Vulink NCC, Hollmann MW, Lamme VAF
625 (2013) NMDA receptor antagonist ketamine impairs feature integration in visual
626 perception. Herzog MH, ed. PLoS ONE 8:e79326.

627 Mierau SB, Patrizi A, Hensch TK, Fagiolini M (2016) Cell-Specific Regulation of N-Methyl-D-
628 Aspartate Receptor Maturation by Mecp2 in Cortical Circuits. Biol Psychiatry 79:746–
629 754.

630 Murphy KM, Balsor J, Beshara S, Siu C, Pinto JGA (2014) A high-throughput semi-automated
631 preparation for filtered synaptoneurosomes. Journal of Neuroscience Methods 235:35–40.

632 Murphy KM, Beston BR, Boley PM, Jones DG (2005) Development of human visual cortex: a
633 balance between excitatory and inhibitory plasticity mechanisms. Dev Psychobiol
634 46:209–221.

635 Owsley C (2011) Aging and vision. VISION RESEARCH 51:1610–1622.

636 Philpot BD, Cho KKA, Bear MF (2007) Obligatory role of NR2A for metaplasticity in visual
637 cortex. Neuron 53:495–502.

638 Philpot BD, Espinosa JS, Bear MF (2003) Evidence for altered NMDA receptor function as a
639 basis for metaplasticity in visual cortex. Journal of Neuroscience 23:5583–5588.

640 Philpot BD, Sekhar AK, Shouval HZ, Bear MF (2001) Visual experience and deprivation
641 bidirectionally modify the composition and function of NMDA receptors in visual cortex.
642 Neuron 29:157–169.

643 Pinto JGA, Hornby KR, Jones DG, Murphy KM (2010) Developmental changes in GABAergic
644 mechanisms in human visual cortex across the lifespan. Front Cell Neurosci 4:16
645 Available at:
646 http://www.frontiersin.org/Journal/Abstract.aspx?s=156&name=cellular_neuroscience&
647 ART_DOI=10.3389/fncel.2010.00016.

648 Pinto JGA, Jones DG, Williams CK, Murphy KM (2015) Characterizing synaptic protein
649 development in human visual cortex enables alignment of synaptic age with rat visual
650 cortex. Front Neural Circuits 9:3.

651 Quinlan EM, Olstein DH, Bear MF (1999a) Bidirectional, experience-dependent regulation of N-
652 methyl-D-aspartate receptor subunit composition in the rat visual cortex during postnatal
653 development. Proc Natl Acad Sci U S A 96:12876–12880.

654 Quinlan EM, Philpot BD, Huganir RL, Bear MF (1999b) Rapid, experience-dependent
655 expression of synaptic NMDA receptors in visual cortex in vivo. Nat Neurosci 2:352–
656 357.

657 Ramoa AS, Mower AF, Liao D, Jafri SI (2001) Suppression of cortical NMDA receptor function
658 prevents development of orientation selectivity in the primary visual cortex. Journal of
659 Neuroscience 21:4299–4309.

660 Rivadulla CC, Sharma JJ, Sur MM (2001) Specific roles of NMDA and AMPA receptors in
661 direction-selective and spatial phase-selective responses in visual cortex. J Neurosci
662 21:1710–1719.

663 Rumpel S, Hatt H, Gottmann K (1998) Silent synapses in the developing rat visual cortex:
664 evidence for postsynaptic expression of synaptic plasticity. J Neurosci 18:8863–8874.

665 Scherzer CR, Landwehrmeyer GB, Kerner JA, Counihan TJ, Kosinski CM, Standaert DG,
666 Daggett LP, Veliçelebi G, Penney JB, Young AB (1998) Expression of N-methyl-D-
667 aspartate receptor subunit mRNAs in the human brain: hippocampus and cortex. J Comp
668 Neurol 390:75–90.

669 Self MW, Kooijmans RN, Supèr H, Lamme VA, Roelfsema PR (2012) Different glutamate
670 receptors convey feedforward and recurrent processing in macaque V1. Proc Natl Acad
671 Sci U S A 109:11031–11036.

672 Sheng M, Cummings J, Roldan LA, Jan YN, Jan LY (1994) Changing subunit composition of
673 heteromeric NMDA receptors during development of rat cortex. Nature 368:144–147.

674 Siu CR, Balsor JL, Jones DG, Murphy KM (2015) Classic and Golli Myelin Basic Protein have
675 distinct developmental trajectories in human visual cortex. Front Neurosci 9:138.

676 Smith GB, Heynen AJ, Bear MF (2009) Bidirectional synaptic mechanisms of ocular dominance
677 plasticity in visual cortex. Philosophical Transactions of the Royal Society B: Biological
678 Sciences 364:357–367.

679 Stocca G, Vicini S (1998) Increased contribution of NR2A subunit to synaptic NMDA receptors
680 in developing rat cortical neurons. The Journal of Physiology 507 (Pt 1):13–24.

681 Taylor G, Hipp D, Moser A, Dickerson K, Gerhardstein P (2014) The development of contour
682 processing: evidence from physiology and psychophysics. Front Psychol 5:719.

683 Turrigiano GG (2008) The self-tuning neuron: synaptic scaling of excitatory synapses. Cell
684 135:422–435.

685 Turrigiano GG (2017) The dialectic of Hebb and homeostasis. Philosophical Transactions of the
686 Royal Society B: Biological Sciences 372:20160258.

687 Turrigiano GG, Nelson SB (2004) Homeostatic plasticity in the developing nervous system. Nat
688 Rev Neurosci 5:97–107.

689 Vicini S, Wang JF, Li JH, Zhu WJ, Wang YH, Luo JH, Wolfe BB, Grayson DR (1998)
690 Functional and pharmacological differences between recombinant N-methyl-D-aspartate
691 receptors. Journal of Neurophysiology 79:555–566.

692 Wang Y, Zhou Y, Ma Y, Leventhal AG (2005) Degradation of signal timing in cortical areas V1
693 and V2 of senescent monkeys. Cereb Cortex 15:403–408.

694 Williams K, Irwin DA, Jones DG, Murphy KM (2010) Dramatic Loss of Ube3A Expression
695 during Aging of the Mammalian Cortex. Front Aging Neurosci 2:18.

696 Yashiro K, Philpot BD (2008) Regulation of NMDA receptor subunit expression and its
697 implications for LTD, LTP, and metaplasticity. Neuropharmacology 55:1081–1094.

698 Yoshii A, Sheng MH, Constantine-Paton M (2003) Eye opening induces a rapid dendritic
699 localization of PSD-95 in central visual neurons. Proc Natl Acad Sci U S A 100:1334–
700 1339.

701 Zhang J, Wang X, Wang Y, Fu Y, Liang Z, Ma Y, Leventhal AG (2008) Spatial and temporal
702 sensitivity degradation of primary visual cortical cells in senescent rhesus monkeys. Eur J
703 Neurosci 28:201–207.

704 Zilles K, Werners R, Büsching U, Schleicher A (1986) Ontogenesis of the laminar structure in
705 areas 17 and 18 of the human visual cortex. A quantitative study. Anat Embryol 174:339–
706 353.

Figure Legends

Figure 1 - Development of PSD-95, GluA2 , and GluN1 expression in human V1. (A) A scatterplot of PSD-95 expression across the lifespan fit with a Gaussian function (R^2=0.457, $p<0.0001$) with peak expression at 9.6 years (+/- 4.1 years). (B) Age-binned results for PSD-95 expression. (C) A scatterplot of GluA2 expression across the lifespan fit with a Gaussian function (R^2=0.131, $p<0.01$), with peak expression at 3.1 years (+/- 1.8 years). (D) Age-binned results for GluA2 expression. (E) A scatterplot of GluN1 expression across the lifespan fit with an exponential decay function (R^2=0.482, $p<0.0001$), and fell to mature levels (3τ) at 4.2 years (+/- 1.7 years). (F) Age-Binned results for GluN1 expression. For the scatterplots, grey dots represent each run, black dots represent the average for each case and age was plotted on a logarithmic scale. For the histograms, protein expression was binned into age groups (< 0.3 years, Neonates; 0.3-1 year, Infants; 1-4 years, Young Children; 5-11 years, Older Children; 12-20 years, Teens; 21-55 years, Young Adults; >55 years, Older Adults) showing the mean and SEM. Representative bands are shown above each age group. (*$p<0.05$, **$p<0.01$, ***$p<0.001$).

Figure 2 - Development of the AMPA:NMDA balance ((GluA2-GluN1)/(GluA2+GluN1)) in human V1. (A) A scatterplot of the AMPA:NMDA balance across the lifespan fit with a quadratic function (R^2=0.406, $p<0.0001$), which peaked at 10.7 years (95% CI 4.8-23.7 years). (B) Age-Binned results for the AMPA:NMDA balance. Scatterplot, histogram and significance levels plotted using the conventions described in Figure 1.

Figure 3 - Development of GluN2B and GluN2A in human V1. (A) A scatterplot of GluN2B expression across the lifespan fit with a Gaussian function (R^2=0.176, $p<0.01$), with peak expression at 1.2 years (+/- 0.7 years). (B) Age-Binned results for GluN2B expression. (C) A

scatterplot of GluN2A expression across the lifespan fit with a weighted curve. (D) Age-Binned results for GluN2A expression. Scatterplots, histograms, and significance levels plotted using the conventions described in Figure 1.

Figure 4 - Development of GluN2B and GluN2A normalized to GluN1 in human V1. (A) A scatterplot of GluN2B expression normalized to GluN1 across the lifespan fit with a Gaussian function (R^2=0.106, $p<0.05$), with peak expression at 3.2 years (+/-1.8 years). (B) Age-Binned results for GluN2B normalized to GluN1 expression. (C) A scatterplot of GluN2A normalized to GluN1 expression across the lifespan fit with a weighted curve. (D) Age-Binned results for GluN2A normalized to GluN1. Scatterplots, histograms, and significance levels plotted using the conventions described in Figure 1.

Figure 5 - Development of the 2A:2B balance ((GluN2A-GluN2B)/(GluN2A+GluN2B)) in human V1. (A) A scatter plot of the 2A:2B balance across the lifespan fit with a Gaussian function (R2=0.633, $p<0.0001$), with peak expression around 35.9 years of age (+/- 4.6 years). (B) Age-Binned results for the 2A:2B balance. Scatterplot, histogram, and significance levels plotted using the conventions described in Figure 1.

Figure 6 - Development of the VMR for PSD-95, GluA2, GluN1, GluN2A, and GluN2B in human V1. Black dots are the VMR for a moving window of 3 cases. Each protein's scatterplot were fit with a Gaussian function, and the data were normalized to the peak of the function. (A) PSD-95 VMR peaked at 2.5 years (+/- 0.5 years) (R2=0.778, $p<0.0001$). (B) GluA2 VMR peaked at 2.1 years (+/- 0.6 years) (R2=0.641, $p<0.0001$). (C) GluN1 VMR peaked at 1.1 years (+/- 0.2 years) (R2=0.8, $p<0.0001$). (D) GluN2A VMR peaked at 1.6 years (+/- 0.4 years) (R2=0.694, $p<0.0001$). (E) GluN2B VMR peaked at 1.1 years (+/- 0.3 years) (R2=0.618,

751 $p<0.0001$). (F) A summary chart showing the progression of peaks of inter-individual variability
752 (vertical black line) and the 95% CI (colored bar) for each protein.

753 Figure 7 - Summary of the 5 stages of development for the glutamatergic proteins. Changes for
754 the individual glutamatergic proteins are illustrated with grey-levels where black represents the
755 maximum expression and lighter grey less expression. GluN1 peaked during the first year (stage
756 1), GluN2B, GluA2, and PSD-95 in late childhood (stage 3), and GluN2A at ~40 years (stage 4)
757 before declining in aging (stage 5). Changes for the 2 indices (2A:2B, GluA2:GluN1) are color-
758 coded. For the 2A:2B balance red indicates more GluN2B and green more GluN2A, and for the
759 AMPA:NMDA balance red indicates more GluN1 and green more GluA2. The shift to more
760 GluN2A peaked in adulthood (stage 4) and then returned to more GluN2B in aging (stage 5).
761 The switch to more GluA2 happned at ~ 1 year and continued until late childhood (stage 3). The
762 waves of inter-individual variability for each protein are present with dark blue identifying
763 maximum variability that occurred in young childhood (stage 2) and lighter blue indicating
764 stages with low variability.

765

766 Table 1 - Human V1 tissue samples

Age	Age Group	Sex	PMI (Hours)
20 days	Neonate	M	9
86 days	Neonate	F	23
96 days	Neonate	M	12
98 days	Neonate	M	16
119 days	Neonate	M	22
120 days	Neonate	M	23
133 days	Infant	M	16
136 days	Infant	F	11
273 days	Infant	M	10
1 year 123 days	Young Children	M	21
2 years 57 days	Young Children	F	21
2 years 75 days	Young Children	F	11
3 years 123 days	Young Children	F	11
4 years 203 days	Young Children	M	15
4 years 258 days	Young Children	M	17
5 years 144 days	Older Children	M	17
8 years 50 days	Older Children	F	20
8 years 214 days	Older Children	F	20
9 years 46 days	Older Children	F	20
12 years 164 days	Teens	M	22
13 years 99 days	Teens	M	5
15 years 81 days	Teens	M	16
19 years 76 days	Teens	F	16
22 years 359 days	Young Adults	M	4
32 years 223 days	Young Adults	M	13

50 years 156 days	Young Adults	M	8
53 years 330 days	Young Adults	F	5
69 years 110 days	Older Adults	M	12
71 years 333 days	Older Adults	F	9
79 years 181 days	Older Adults	F	14

767

768 Table 1. Human V1 tissue samples used in this study. Each case is identified by their age in years

769 and days, age group assignment, sex, and post-mortem interval (PMI).

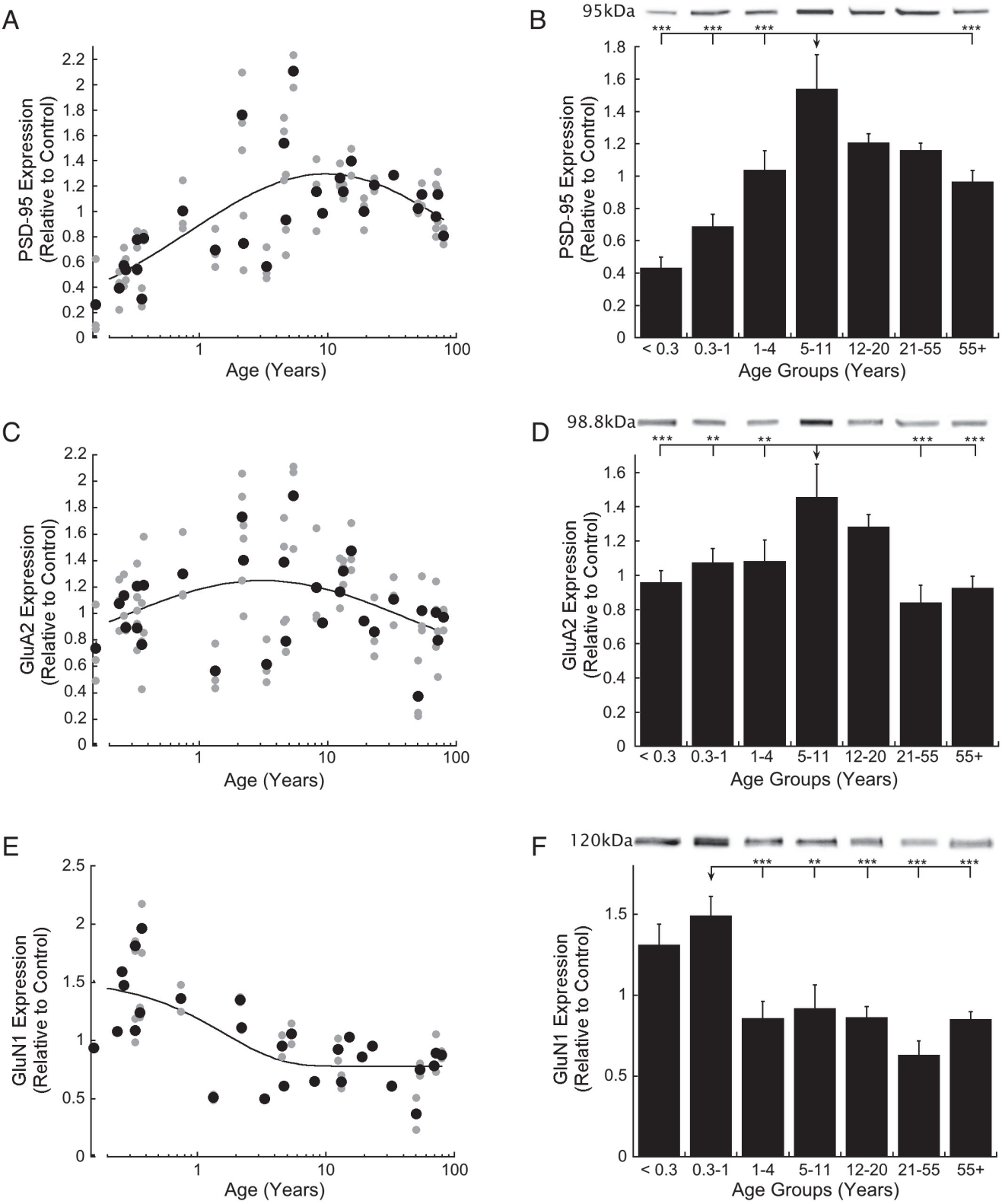

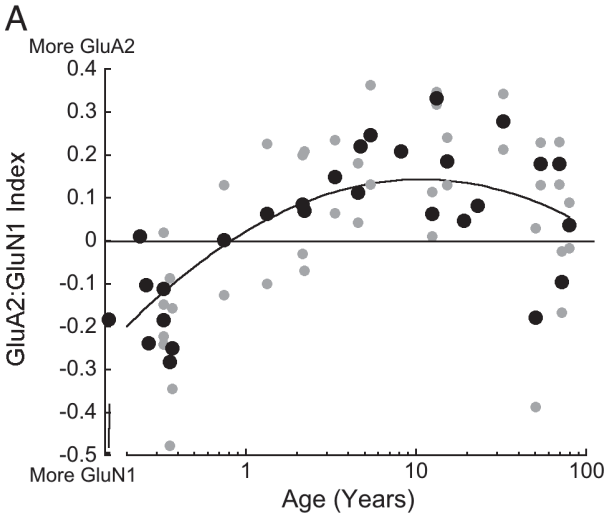

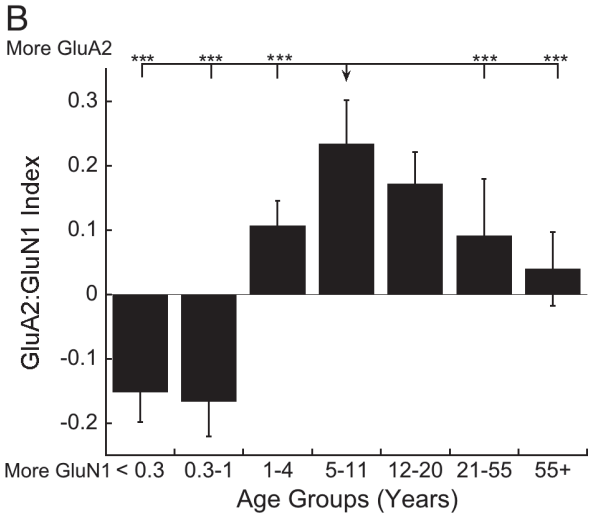

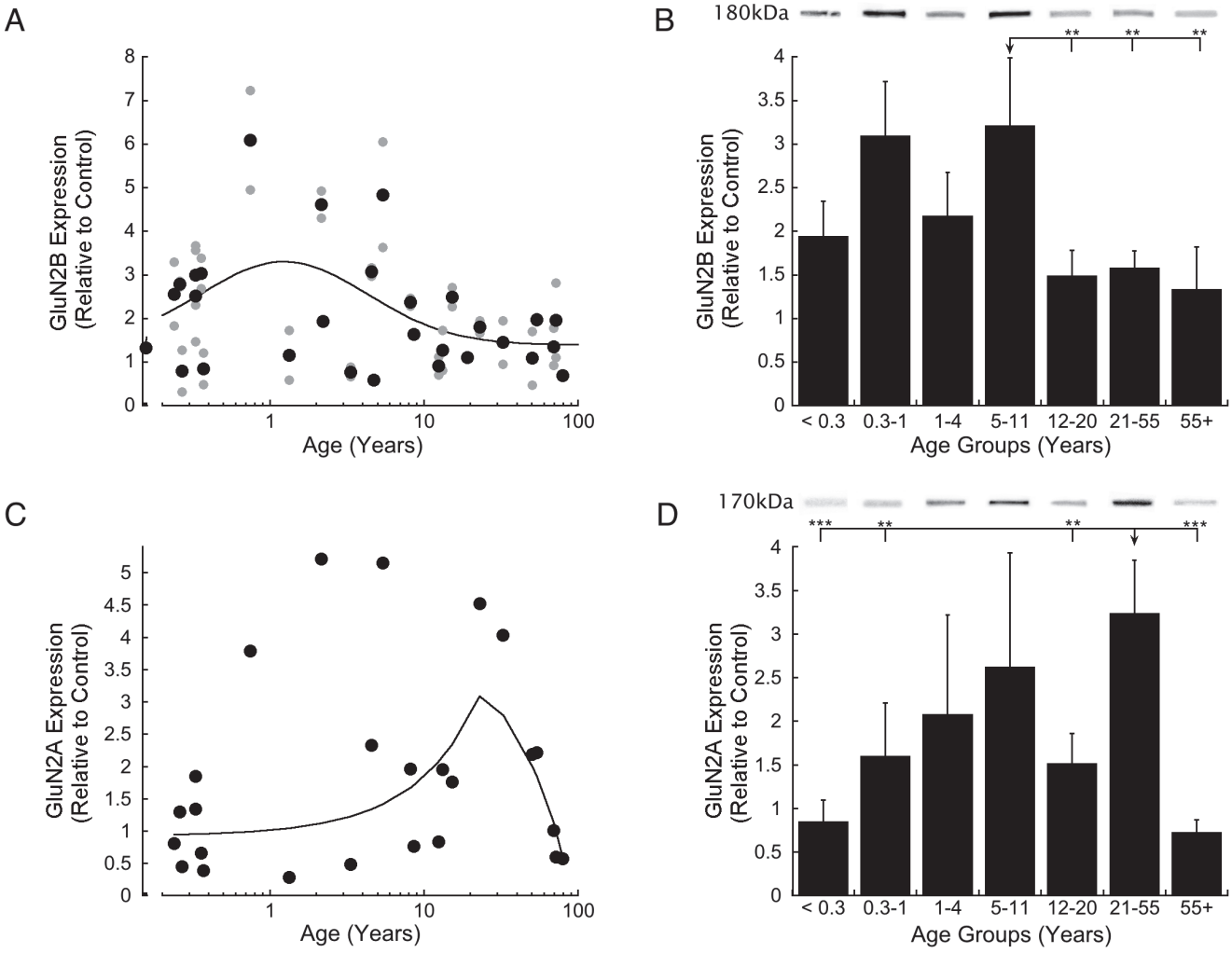

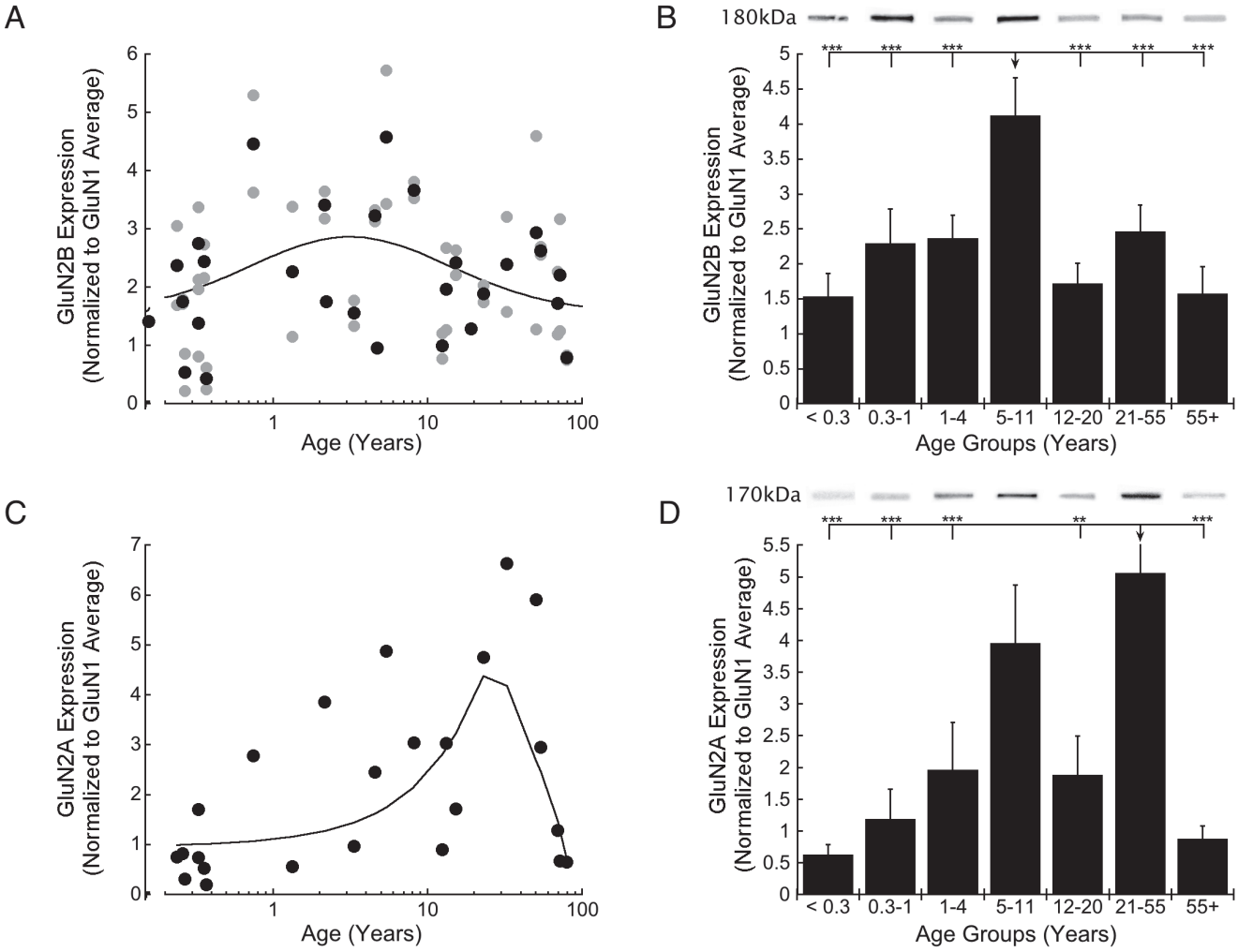

A

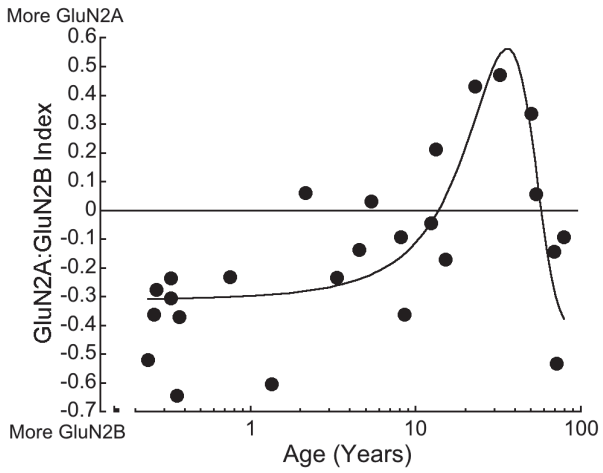

B

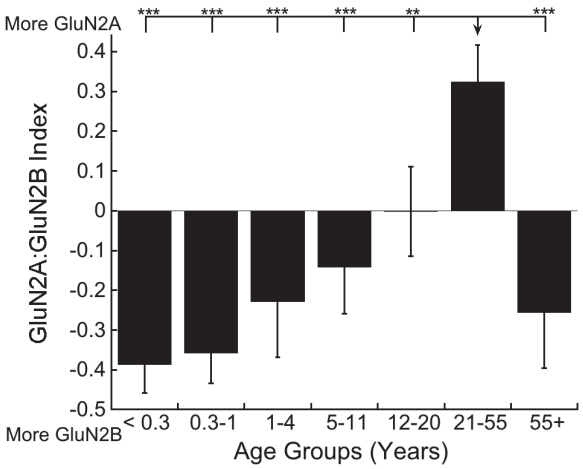

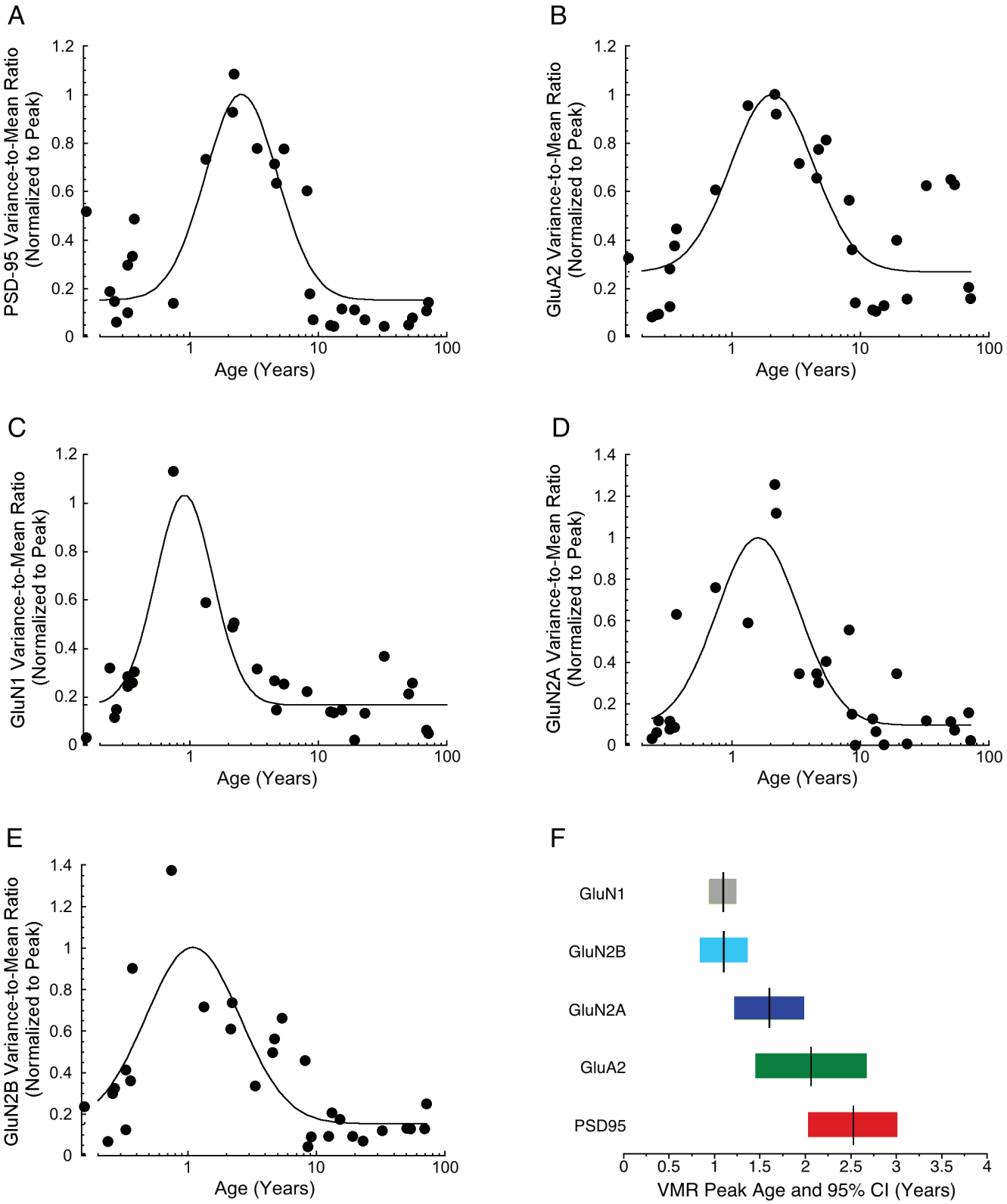

		Stage 1 (<1 year)	Stage 2 (1-4 years)	Stage 3 (5-11 years)	Stage 4 (12-55 years)	Stage 5 (>55 years)
Individual Protein Development	GluN1	GluN1				
	GluN2B			GluN2B		
	GluA2			GluA2		
	PSD-95			PSD-95		
	GluN2A				GluN2A	
Index Development	2A:2B	GluN2B			GluN2A	GluN2B
	GluA2:GluN1	GluN1		GluA2		
Inter-Individual Variability Waves	GluN1		GluN1			
	GluN2B		GluN2B			
	GluA2		GluA2			
	PSD-95		PSD-95			
	GluN2A		GluN2A			